ELECTRON TECHNOLOGY
ISSN 1897-2381
http://www.ite.waw.pl/etij/
Internet Journal

COMPARATIVE STUDY OF SENSOR AND MATERIAL PROPERTIES ON $In_{0.53}Ga_{0.47}As/InP$ FABRICATED BY MBE AND MOCVD

A. WOLKENBERG, T. PRZESŁAWSKI

Institute of Electron Technology, al. Lotników 32/46, 02-668 Warszawa, Poland

Received September 2, 2005; modified December 8, 2005; published December 23, 2005

ABSTRACT

We report the galvanomagnetic properties of Hall and magnetoresistor cross-shaped sensors with lateral dimensions 2 x 3 mm. The comparative study of epi-layers fabricated by MBE and MOCVD are presented. The measured parameters of these devices gave an interesting insight into their behaviour at temperatures ranging from LHe to room temperature. The large changes of the galvanomagnetic parameters vs. magnetic field and temperature allow these devices to be used as field or temperature sensors.

1. Introduction

Hall and magnetoresisitive probes have been employed for studying magnetic properties of various materials for several decades. Most recently, advances in microtechnology have allowed fabrication of such sensors of micron size and they were successfully applied [1], [2].

In recent years an increase of interest can be observed in magnetic field sensors (MFS) which are applied to measurements and monitoring of many changes in physical and mechanical properties. This especially concerns to thin film sensors [3–6].

The aim of this paper is to project a magnetic field sensor built from epitaxial layers of $In_{0.53}Ga_{0.47}As/$ $/InP$ obtained with MBE and MOCVD technology. A comparison of results obtained with these two materials on sensor and material properties is presented.

This device when used as a magnetic field sensor can be adopted for the fields as low as 1 mT and higher. Sensors built from semiconductor with concentration $\sim 1.10^{20}$ m^{-3} can be used at much higher sensitivity but with significant temperature dependence. If we use the $In_{0.53}Ga_{0.47}As$ layer with $n \sim 1–10 \cdot 10^{22}$ m^{-3} then the electrical characteristics are almost independent of temperature. From Hall voltage the sensitivity is 140 mV/0.05 T·6 V. That only is a little smaller than for deep quantum well Hall element (DQW) with sensitivity 300 mV/ /0.05 T·6 V [7–9].

On the basis of our previously reported results obtained for the VdP structure (with $w/l = 1$) [10], [11] we consider that it is possible to obtain sensors using Hall effect with absolute sensitivity $\gamma_0 \sim 1$ V/T and current sensitivity ~ 5600 Ω/T at $B = 0.6$ T and $t = 4$ μm, $n_H = 2.25\ 10^{20}$ m^{-3}, $\mu_H = 0{,}7$ m^2/V at $T \sim 300$ K. For higher concentration $n_H \sim 8.5 \cdot 10^{23}$ m^{-3} and mobility $\mu_H \sim 0{,}5$ m^2/V·s with $t = 1$ μm we have $\gamma_0 \sim 0{,}003$ V/T and $\gamma \sim 5$ Ω/T.

For sensors using the Gauss effect $S_I \sim 800$ Ω/T and $S_V \sim 0{,}5$ (T^{-1}) at $B = 0.6$ T with $t = 4$ μm and $n_H =$ $= 2{,}25 \cdot 10^{20}$ m^{-3} and $\mu_H = 0{,}7$ m^2/V·s. For higher concentration $n_H \sim 8.5 \cdot 10^{23}$ m^{-3} and $\mu_H \sim 0{,}5$ m^2/V·s with $t = 1$ μm we have $S_I \sim 1$ Ω/T and $S_V \sim 0.05$ (T^{-1}).

In a real semiconductor wafer resistance and sensitivity are dependent on the geometrical shape and magnetic induction B. Magnetoresistors are mainly made in the form of rectangular plates with dimensions described by longitude – l, and width – w. Commonly $l \leq w$ and then resistance R_{xx} of such a device is [12], [13]:

$$R_{xx}(B) = R_{xx}(B=0)[1 + g(w/l)\,(\rho_{xy}/\rho_{xx})^2]\,(\rho_{xx}(B)/\rho_{xx}(0)). \tag{1}$$

In the case of low Hall angles $\theta < \pi/8$ or $\rho_{xy}/\rho_{xx} <$ < 0.4:

$$R_{xx}(B) = R_{xx}(B=0)[1+g(w/l)\,\mu_H^2 B^2]\,(\rho_{xx}(B)/\rho_{xx}(0)). \tag{2}$$

The factor $(\rho_{xx}(B)/\rho_{xx}(0))$ is known as intrinsic magnetoresistance, while $[1 + g(w/l)\ (\mu_H^2 B^2)]$ describes the influence of the shape of the device. The function $g(w/l)$ was calculated by Lippman and Kuhrt [14]. The values of l, w and t which have an influence on magnetoresistance may be presented as follows:

$$R_{xx} = \rho_{xx} \frac{l}{w \cdot t} R\left(\theta, \frac{l}{w}\right). \quad (3)$$

To obtain the largest values of primary resistance the gaussotrons (N_R) are connected in series. Gaussotrons connected in this way have largest current sensitivity S_I [12], [13]:

$$S_I = \frac{dV}{IdB} = \frac{dR(B)}{dB} \quad [\Omega/\mathrm{T}] \quad (4)$$

and voltage sensivity S_V:

$$S_V = \frac{dV}{VdB} = \frac{dR}{RdB} \quad [\mathrm{T}^{-1}]. \quad (5)$$

Heremans presents the solution to the calculations of the influence of the value of l/w on R and G_H by $\Theta \to 0$ and $\Theta \to \infty$ [12], [13], which was used for our structure in Eqs. (6)–(9) and (11). For

$$S_I = \frac{\mu_H \cdot B \cdot N_R \cdot l}{n_H \cdot e \cdot t \cdot w}\left(1 - 0.54\frac{l}{w}\right), \quad (6)$$

$$S_V = \left(1 - 0.54\frac{l}{w}\right)\mu_H^2 \cdot B^2 \quad (7)$$

and if $\mu_H \cdot B > 1$

$$S_I = \frac{N_R}{n_H \cdot e \cdot t} \quad (8)$$

where:

$$N_R = 1,$$

$$S_V = \frac{\mu_H}{\mu_H \cdot B - 3.9 + 5.9\frac{l}{w}}. \quad (9)$$

2. Characteristic parameters of Hall and Gauss devices

Figure 1 presents the dimensional symbols used in the paper [15]. With these symbols we have:

$$U_H = \gamma \cdot I \cdot B \quad (10)$$

where: $\gamma = (R_H/t) \cdot G_H$ – current sensititvity, R_H – Hall constant, t – thickness of the active semiconductor layer, I – polarisation current, B – magnetic induction.

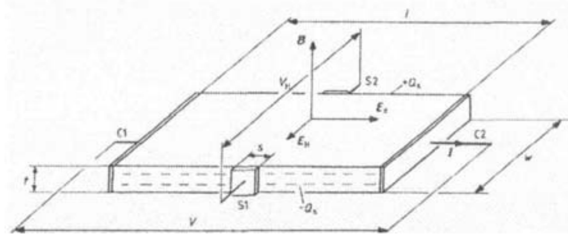

Fig. 1. Rectangular Hall structure.

To measure the exact Hall voltage U_H the relation l/w should have the value of more than 4, then $U_H \to$ $\to U_{H\infty}$. The relation between $U_H/U_{H\infty}$ is defined as the geometrical factor for the Hall effect in the rectangular device:

$$G_H = U_H/U_{H\infty} \quad (10a)$$

where: U_H – measured Hall voltage, $U_{H\infty}$ – Hall voltage measured in a rectangle with $l = \infty$ ($G_H = 1$).

Calculation of the geometrical factor for the Hall effect in a cross-shaped device (Fig. 2) is possible using the Haeusler-Lipmann procedure [16]:

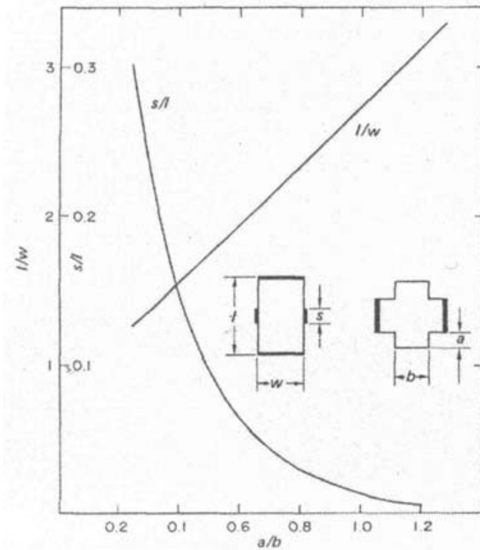

Fig. 2. Nomogram for a cross-shaped device after Haeusler and Lippman [16].

$$G_H = \left[1 - \exp\left(-\frac{\pi}{2}\cdot\frac{l}{w}\right)\cdot\left(\frac{\Theta}{\tan\Theta}\right)\right]\cdot\left[1 - \frac{2}{\pi}\cdot\frac{s}{w}\frac{\Theta}{\tan\Theta}\right] \quad (11)$$

where: $\tan\Theta = \mu_H B$, s – voltage electrode width, l/w = = 1.7 for our cross-structure with a/b = 0.5. On applying the nomogram in Fig. 2 to obtain G_H for a cross-shaped structure we first take a/b = 0.5 (a = = 1 mm, b = 2 mm) and then l/w = 1.71 and l = = 1.71 w. For s/l = 0.1 we have $s/(1.71 \cdot w)$ = 0.1 and s/w = 0.171. Thereafter having all parameters, we can determine the value of G_H for our cross-shaped structure (see Figs. 4a–c) of the two materials, i.e. 273MBE and 3017MOCVD (Table 1). To prove the reliability of the cross-shaped structure, the physical properties of both materials are determined using VdP

structure also (Table 1). We can see that the concentration, mobility and resistivity measurements are comparable using cross-shaped and VdP structure. Crystallographic properties of these materials have been investigated by the XRD method. The results are presented in Figs. 3a–c. On inspecting these results we can establish that the differences of lattice constants are consisted with small differences in chemical composition of the $In_{0.53}Ga_{0.47}As$ on InP layers. The 273MBE structure has the composition $In_{0.533}Ga_{0.467}As$ and structure 3017MOCVD – $In_{0.5312}Ga_{0.4688}As$.

Table 1. Basic parameters of the samples at T = 300 K, B = 0.6 T

No	Sensor shape	Metallurgical thickness t [μm]	Concentration n_H [m^{-3}]	Mobility μ_H [m^2/V·s]	Resistivity ρ_B [Ω m]	Lattice constant disorder [degree]
273 MBE	Cross-shaped VdP	7.0	$1.8\cdot10^{20}$ $2.2\cdot10^{20}$	0.7 0.7	0.043 0.052	0.032
3071 MOCVD	Cross-shaped VdP	3.0	$1.6\cdot10^{21}$ $1.6\cdot10^{21}$	1.0 1.0	0.0032 0.0032	0.013

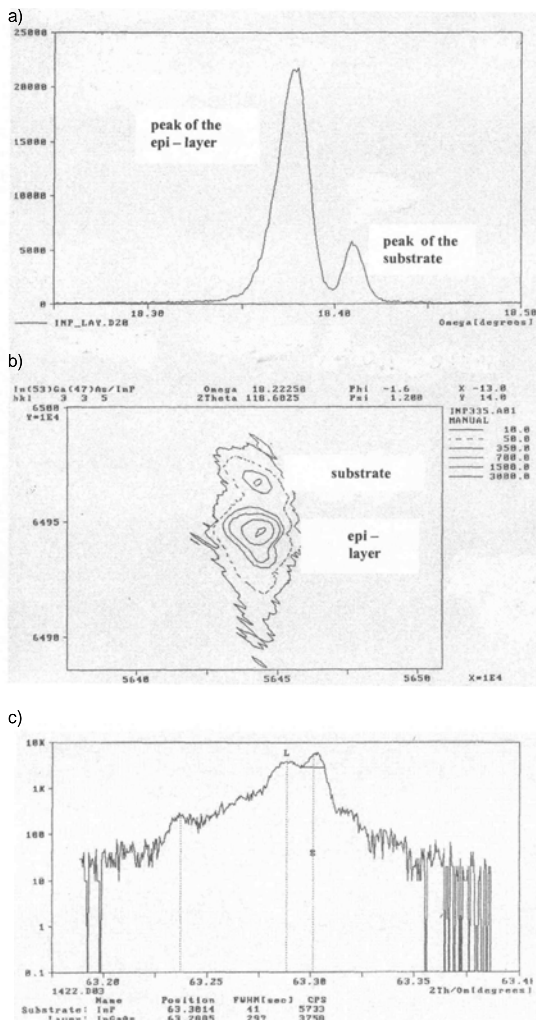

Fig. 3. XRD results of 273MBE (a, b) and 3017MOCVD (c).

The difference in the In/Ga ratio may be responsible for the measured galvanomagnetic properties of the devices. This small deviation from the matched structure may lead to tensions on the interface between $In_{0.53}Ga_{0.47}As$ and InP with important consequences for the electrical behaviour of the whole sensor structure.

3. Sensors construction and parameters

The sensors whose properties are described in the paper are presented in Fig. 4a–c. Figure 4a shows the layout of the mask and 4b and c show the whole sensor and a part of sensor, respectively. All galvanomagnetic parameters were measured on such devices in the configuration as a Hall device and as Gauss device. The obtained results were as follows.

In Fig. 5 is presented the magnetic induction B dependence of G_H and in Fig. 6 its temperature dependence at three magnetic fields. Figures 7 and 8 show the dependence on B and temperature of the product $\mu_H B = \tan\Theta$, respectively. Geometrical factor G_H is for both layers (MBE and MOCVD) dependent on magnetic induction B at all investigated temperatures (Figs. 5a and b). Maximum possible value of G_H is 1 and this can be obtained little earlier by the MOCVD structure (Fig. 5b). G_H from temperature is independent only at the lowest B values (Figs. 6a and b). The MBE structure at higher B values shows non linear dependence on temperature (Fig. 6a). The MOCVD structure shows G_H independent on temperature at temperatures lower as 70 K for higher values of B (Fig. 6b). Dependence of $\tan\Theta$ on magnetic induction B (Figs. 7a and b) shows that only at the B lower as 0.2 T we could calculate the properties by low field approach. Dependence of $\tan\Theta$ on temperature (Figs. 8a and b) shows that $\tan\Theta$ values are constant at all temperatures only for $B \leq 0.04 - 0.05$ T. G_H values are important by calculation of γ in Hall structures (Eq. 13). Above mentioned remarks described the area of possible applying of presented here calculations.

The key parameters of the Hall structures are the sensitivities [17–24]:

- absolute sensitivity connected with the maximum output voltage:

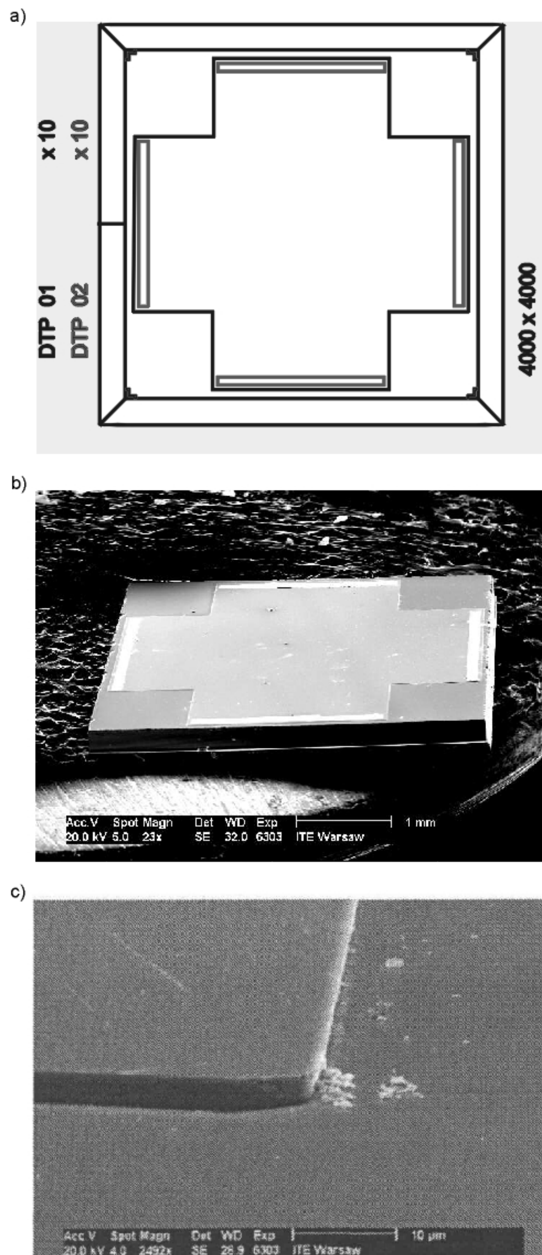

Fig. 4. Mask layout for cross-shaped sensor (a), the sensor structure after etching (b), a part of sensor from b (c).

$$\gamma_0 = \frac{U_{H,\max}}{B} \quad [\text{V/T}], \tag{12}$$

- current sensivity described as Hall voltage for unit polarisation current and unit magnetic induction:

$$\gamma = \frac{V_H}{I \cdot B} = G_H \frac{R_H}{t} \quad [\Omega/\text{T}] \tag{13}$$

where: U_H – Hall voltage [V], I – polarisation current [A], B – perpendicular part of magnetic induction [T], G_H – geometrical factor for cross-shaped Hall structure (Eq. (11)), R_H – Hall factor [C·m^{-3}], t – thickness of active part of the structure [μm].

The sensitivities γ_0 and γ are presented in Figs. 9–12. The absolute sensitivity γ_0 of MBE probe working as Hall structure (Fig. 9a) is independent on B only at

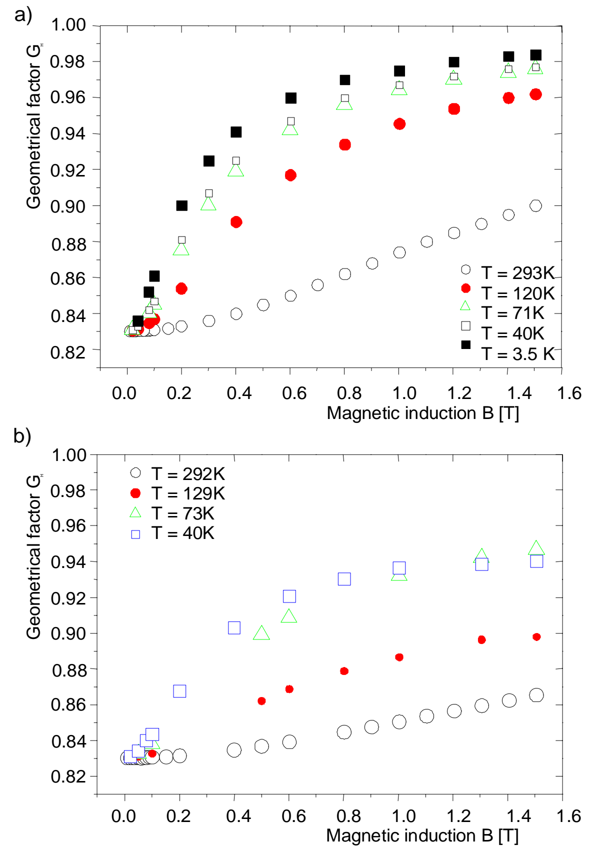

Fig. 5. The function G_H vs. magnetic induction B: a) MBE273, b) 3017MOCVD.

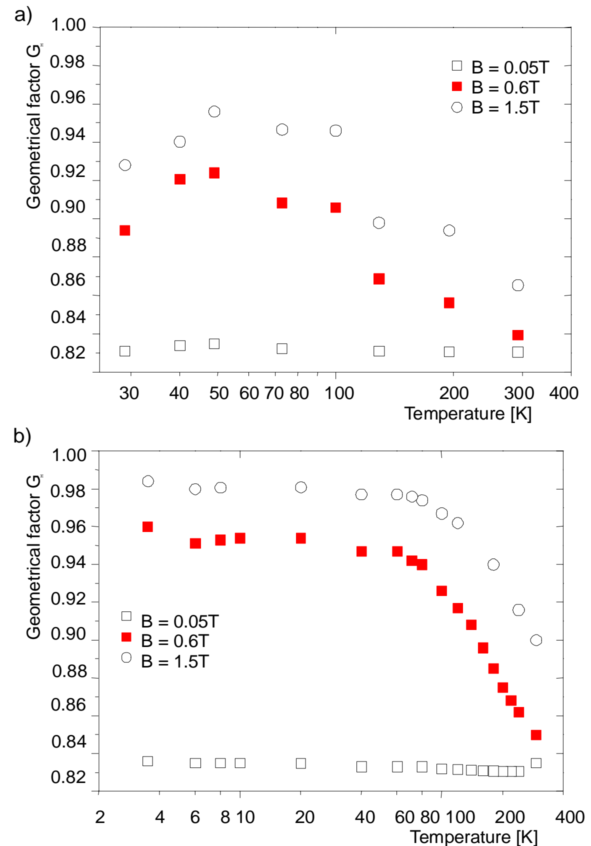

Fig. 6. The function G_H vs. temperature: a) MBE273, b) 3017MOCVD.

300 K, at lower temperatures that dependence is significant. In contrary the MOCVD probe working also as Hall structure shows nearly constant γ_0 at all B

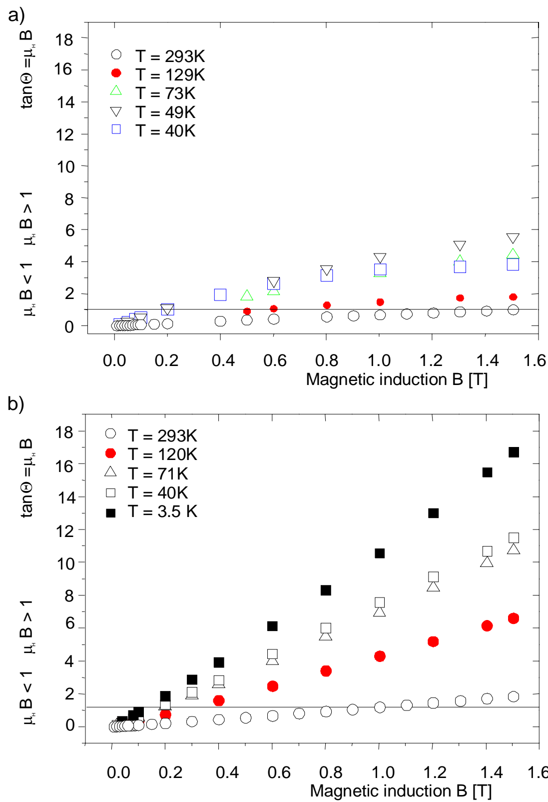

Fig. 7. Dependence of tanΘ on magnetic induction, continuous line marks the value for $\Theta = 45^o$: a) 273MBE, b) 3017MOCVD.

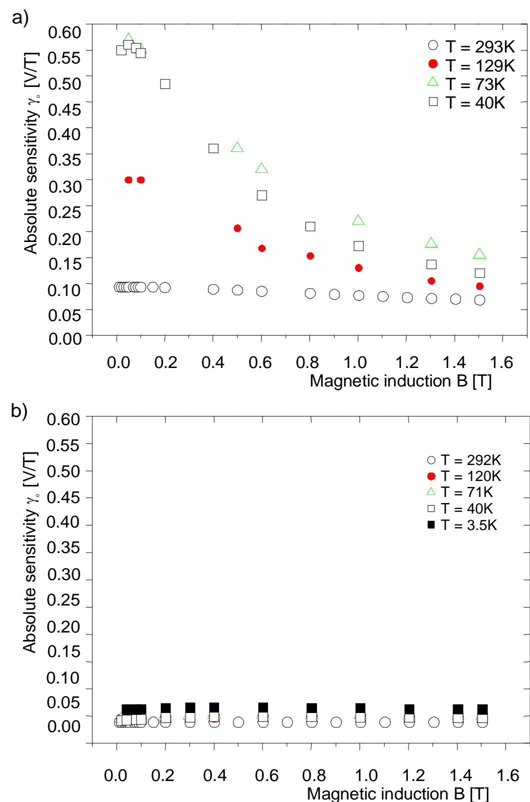

Fig. 9. Absolute sensitivity of Hall structure vs. magnetic induction *B*: a) 273MBE, b) 3017MOCVD.

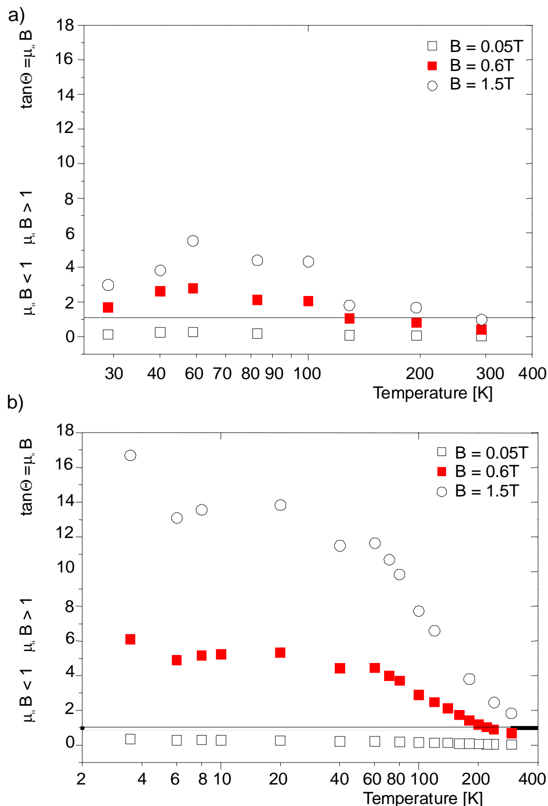

Fig. 8. Dependence of tanΘ on temperature, continuous line marks the value for $\Theta = 45^o$: a) 273MBE, b) 3017MOCVD.

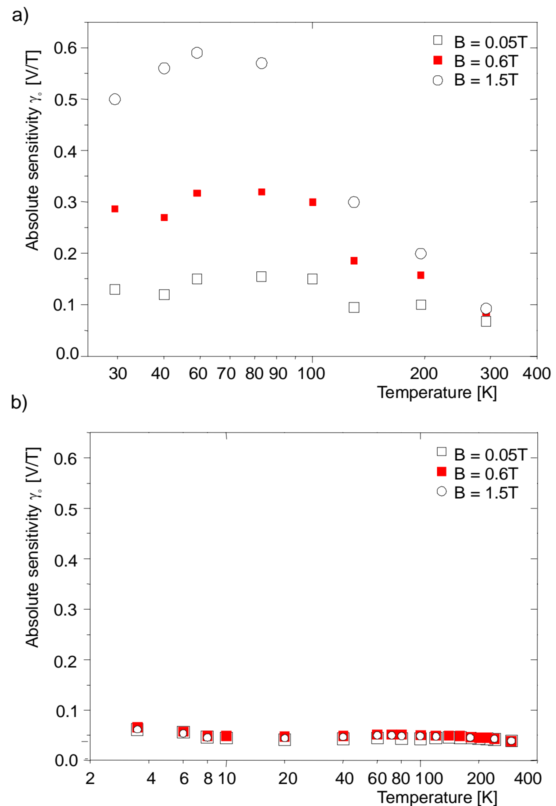

Fig. 10. Absolute sensitivity of Hall structure vs. temperature: a) 273MBE, b) 3017MOCVD.

and temperatures (Fig. 9b). Analogic behaviour of γ_0 show the structures from MBE and MOCVD (Figs. 10a and b) in dependence vs. temperature. The Eq. (12) shows that we can say that more flat curves of γ_0 are the consequence of lower value of measured U_H.

Current sensitivities γ of Hall structures show important differences between MBE and MOCVD

layers (Figs. 11 and 12). The Hall structures from MOCVD present constant value of γ at different magnetic induction and temperature. That is in

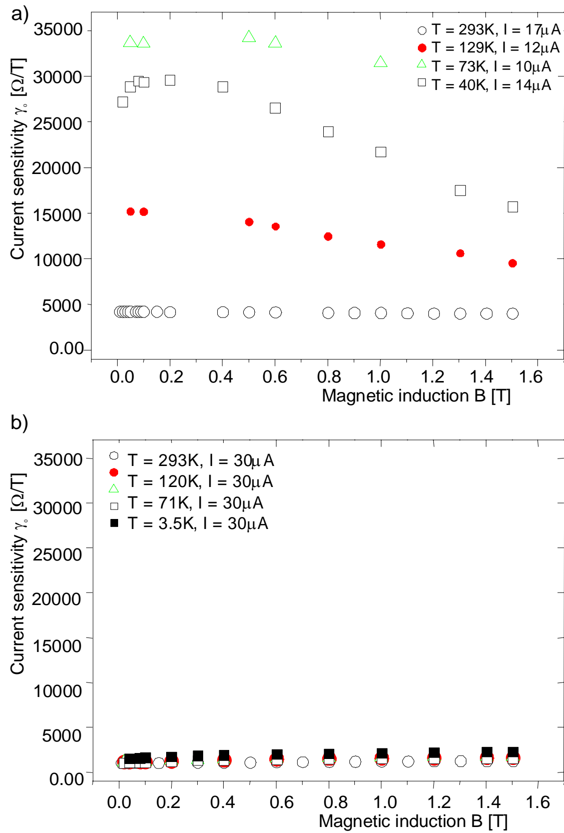

Fig. 11. Current sensitivity γ of Hall structure vs. magnetic induction B: a) 273MBE, b) 3017MOCVD.

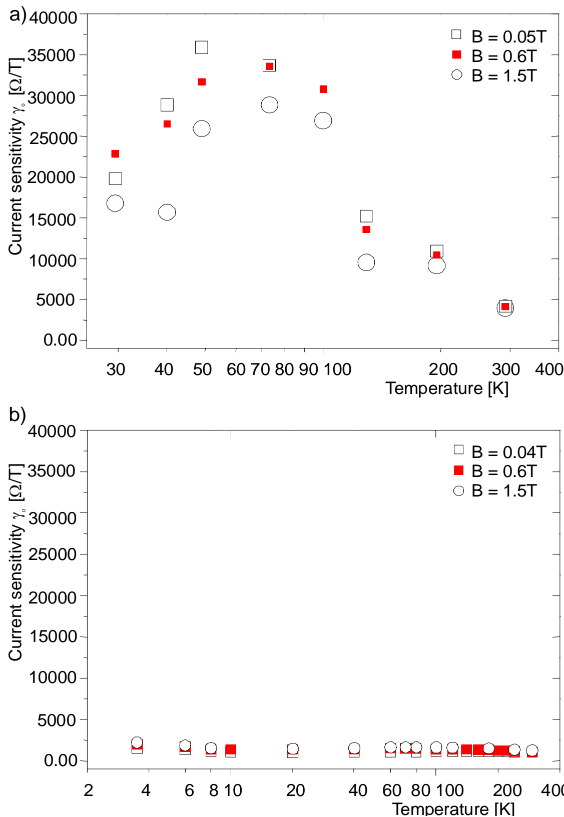

Fig. 12. Current sensitivity γ of Hall structure vs. temperature: a) 273MBE, b) 3017MOCVD.

contrary to MBE layer which has constant values of γ independent on B only at 300 K (Fig. 11a). The Eq. (13) shows that we can say that more flat curves of γ are the consequence of lower value of measured R_H.

Similar discussion can be done for cross-shaped structures (Figs. 13–16). Their properties as magnetoresistance sensors are not very different between MBE and MOCVD layers. They all present flat current sensitivity at higher magnetic induction (Fig. 13) and temperature independent current sensitivity has only MOCVD cross-shaped structure (Fig. 14b). Voltage sensitivity vs. magnetic field and temperature of cross-shaped structures have only at limited area flat sensitivity curves (Figs. 15 and 16).

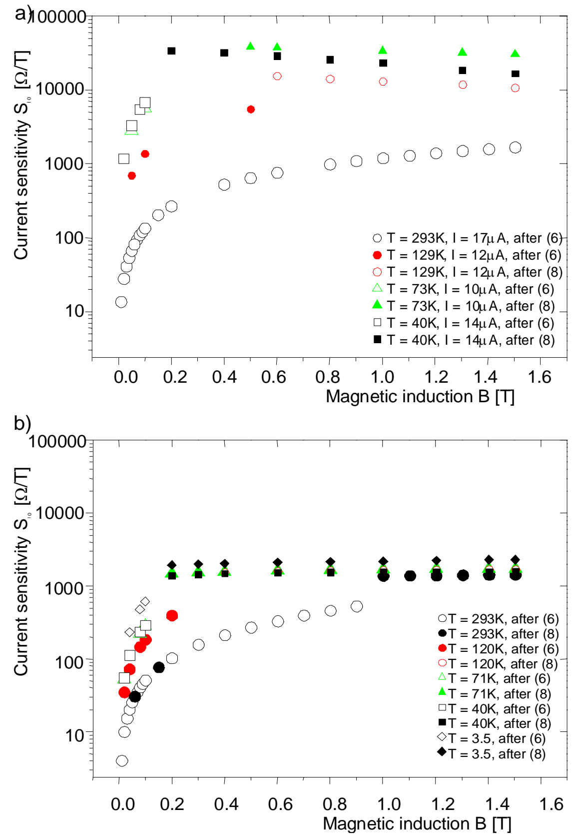

Fig. 13. Current sensitivity of the cross-shaped structure working as a magnetoresistance sensor vs. magnetic induction: a) 273MBE, b) 3017MOCVD.

We now proceed to describe the galvanomagnetic properties of our structure working as a Gauss device. Figures 13–16 present the current and voltage sensitivities for operation as resistors derived for low field from Eqs. (6), (7) and for high fields from Eqs. (8), (9).

Input power of sensor is calculated from equation [25–27]:

$$P_X = (I_X)^2 \cdot R_X = (I_X)^2 \cdot \rho \frac{l}{w \cdot t} \qquad (14)$$

and the theoretical efficiency is given by [25 – 27]:

$$\eta = \frac{R_H^2 \cdot B^2}{4\rho^2 \zeta} = 0.34 \cdot 10^{-16} \frac{(\mu_H B)^2}{\zeta} \qquad (15)$$

where: ζ – coefficient connected with spreading current between the Hall electrodes, practically $\zeta = 2 - 5$.

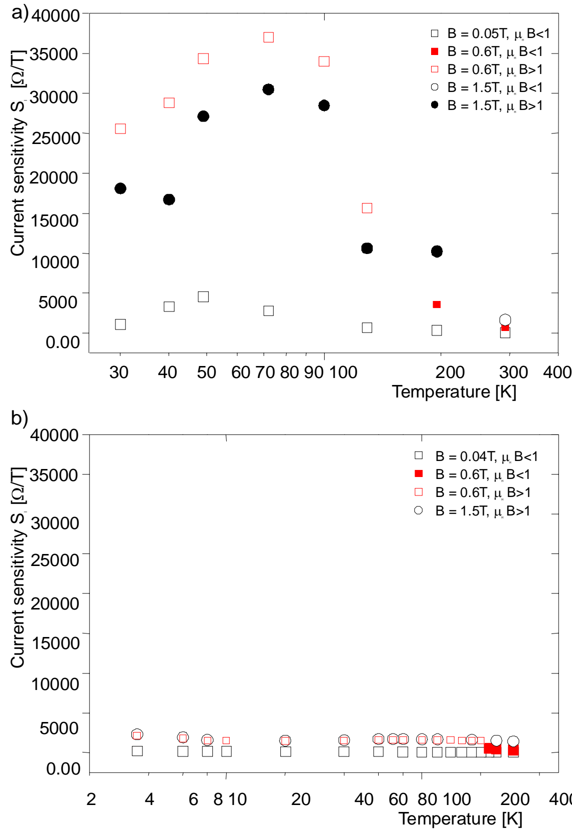

Fig. 14. Current sensitivity of the cross-shaped structure working as a magnetoresistance sensor vs. temperature: a) 273MBE, b) 3017MOCVD.

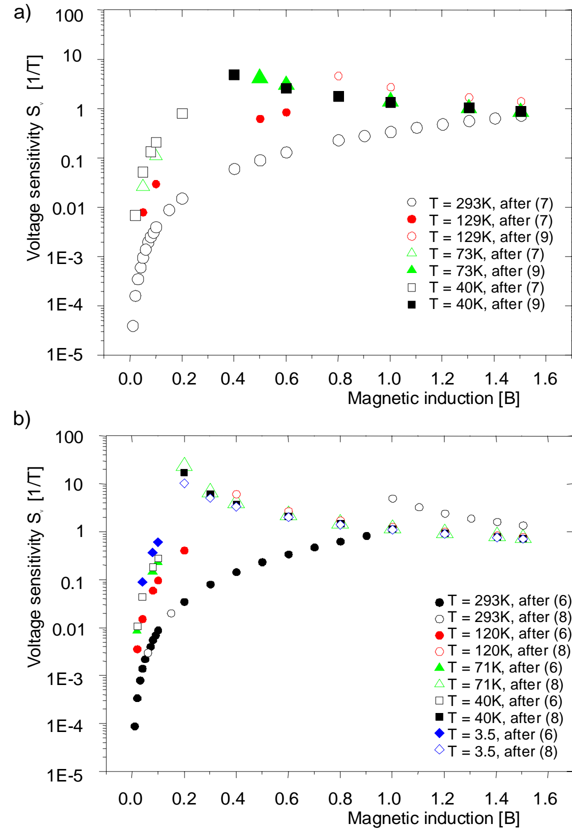

Fig. 15. Voltage sensitivity of the cross-shaped structure working as a magnetoresistance sensor vs. magnetic field: a) 273MBE, b) 3017MOCVD.

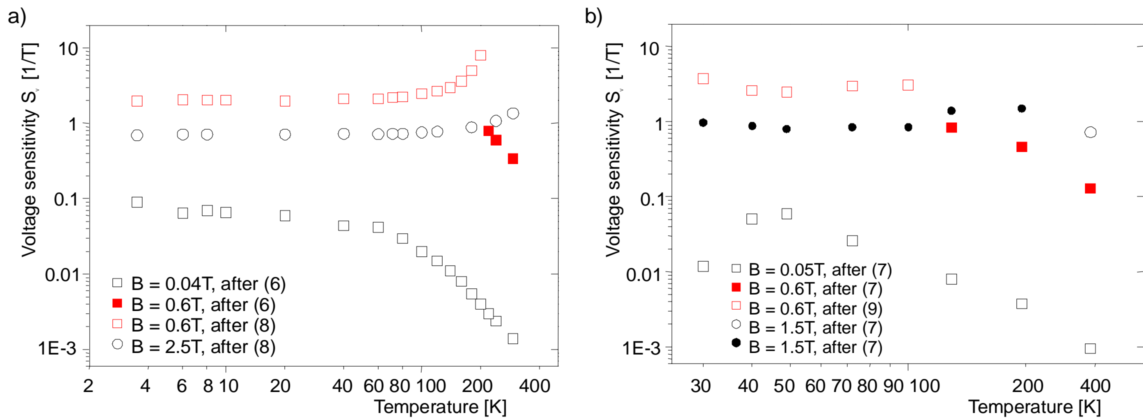

Fig. 16. Voltage sensitivity of the cross-shaped structure working as a magnetoresistance sensor vs. temperature: a) 273MBE, b) 3017MOCVD.

The basic electrical parameters of the sensor built from 273MBE are presented in Table 2 and of that from 3017MOCVD in Table 3. In these tables are presented the results obtained at room temperature and at 40 K for 273MBE and at 3.5 K for 3017 MOCVD.

Table 2. Electrical parameters of sensors built from 273MBE working as Hall and Gauss device

T [K]	B [T]	I [μA]	P_X [μW]	R_X [Ω]	R_H [$m^3 \cdot C^{-1}$]	γ_0 [$V \cdot T^{-1}$]	γ [$\Omega \cdot T^{-1}$]	S_I [$\Omega \cdot T^{-1}$]	S_V [T^{-1}]	$\Delta\rho/\rho_0$ [%]	$\mu_H B$	$\eta_{theoret.}$ [%]
293	0.6	17	2	7000	0.0345	0.085	4140	765	0.13	7	0.425	1.5
	1.5				0.032	0.068	4000	1682	0.73	26	0.997	8.4
40	0.6	14	3.0	6550	0.2	0.27	26556	28840	2.6	130	2.64	60
	1.5				0.13	0.12	15730	16727	0.88	240	3.85	–

P_X – input power; R_X – input resistance; R_H – Hall factor; γ_0 – absolute sensitivity of Hall device; γ – current sensitivity of Hall device; S_I – current sensitivity of Gauss device; S_V – voltage sensitivity of Gauss device; $\Delta\rho/\rho_0$ – relative increase of resistivity of Gauss device; η – theoretical efficiency (for scattering on thermal vibrations of crystal lattice); t = 7 μm – thickness of $In_{0.53}Ga_{0.47}As$ layer

Table 3. Electrical parameters of sensors built from 3017MOCVD working as a Hall and Gauss device

T [K]	B [T]	I [μA]	P_X [μW]	R_X [Ω]	R_H [$m^3 \cdot C^{-1}$]	γ_0 [$V \cdot T^{-1}$]	γ [$\Omega \cdot T^{-1}$]	S_I [$\Omega \cdot T^{-1}$]	S_V [T^{-1}]	$\Delta\rho/\rho_0$ [%]	$\mu_H B$	$\eta_{theoret.}$ [%]
293	0.6	30	1.0	1160	0.004	0.04	1128	332	0.342	5	0.68	4
	1.5				0.0045	0.04	1287	1430	136	18	1.85	30
3.5	0.6	30	0.2	207	0.0063	0.066	2027	2112	2.0	70	6.13	–
	1.5				0.007	0.62	2260	2295	0.7	160	16.7	–

P_X – input power; R_X – input resistance; R_H – Hall factor; γ_0 – field sensitivity of Hall device; γ – current sensitivity of Hall device; S_I – current sensitivity of Gauss device; S_V – voltage sensitivity of Gauss device; $\Delta\rho/\rho_0$ – relative increase of resistivity of Gauss device; η – theoretical efficiency (for scattering on thermal vibrations of crystal lattice); t = 3 μm – thickness of $In_{0.53}Ga_{0.47}As$ layer

3. Discussion

The results are presented of electrical characterisation of two cross-shaped galvanomagnetic sensor structures 273MBE with $n_H = 1.8 \cdot 10^{20}$ m^{-3} and 3017MOCVD with $n_H = 1.6 \cdot 10^{21}$ m^{-3}. These can work depending on connection, as a Hall or a magnetoresistor device. It was found that the geometrical function G_H for the Hall device depends on carrier concentration, magnetic field and temperature (Figs. 5 and 6). G_H values are more flat at higher B and lower temperature (Figs. 5 and 6). Similar behaviour was found for the angle θ (tanΘ = $\mu_H B$) and absolute sensitivity γ_0 with current sensitivity γ (Figs. 7–12). In Figs. 7 and 8 is marked the limit between low field approximation $\mu_H B < 1$ and high field when $\mu_H B > 1$. From Figs. 9–12 we can characterise the usefulness of the two investigated materials to work as sensors. Magnetoresistive behaviour of our cross-shaped sensors is presented in Figs. 13 and 14. Current sensitivity is better for the 273MBE layer which is more pure than 3017MOCVD, but the latter has better voltage sensitivity S_V. Presented behaviour also show usefulness of each material as magnetoresistive sensor. Theoretical efficiency (Eq. (15)) in Tables 2 and 3 is calculable only at weak fields approximation (see Figs. 7 and 8). Therefore when μB value in our case is larger as 3.45 then $\eta_{theoret.}$ is impossible to evaluate by Eq. (15). Such behaviour confirms our previous assumption that for galvanomagnetic sensors the purest $In_{0.53}Ga_{0.47}As$ layers are more useful.

All measurements in magnetic field were performed in the fields perpendicular to the sensor surface ($B \perp I$). The angle sensitivity of the sensors was close to theoretical because between perpendicular ($B \perp I$) and parallel ($B \parallel I$) configuration the difference is near 30:1 (directional sensitivity) [28]. Such behaviour allows the sensor to be used as a position sensor.

Summarising the results, we have presented interesting data concerning the behaviour of our sensors at different values induction B and of temperature and we can propose to use this design as a sensor:

- for measurements of position at room temperatures,
- for measurements of magnetic induction at temperatures 40 K – 100 K.

Acknowledgements

This work is supported by the State Committee for Scientific Research under grant No 4T11B 066 22. The authors want to thank Prof. M. Bugajski and Dr Kaniewski for stimulating discussions, Dr A. Jasik (ITME) and Prof. K. Regiński (ITE) for samples preparation, Dr J. Bąk-Misiuk (Institute of Physics, Polish Academy of Sciences) for XRD measurements.

References

1. U. Dibbern, *Magnetic Field Sensors Using the Magnetoresistive Effect*, Sensors a. Actuators, 1986, **10,** 127–140.
2. Yoshinobu Sugiyama, *Recent Progress on Magnetic Sensors with Nanostructures and Applications*, J. Vacuum Sci. Technol. B, 1995, **13**, 1075–1083.
3. R. Kyburz, J. Schmidt, R. S. Popovic, *Highly Sensitive $In_{0.53}Ga_{0.47}As$/InP Hall Sensors Grown by MOVPE*, IEEE Trans. on Electron Dev., 1994, **41**, 315–320
4. G. Vértesy, A. Gasparics, J. Szöllősy, *High Sensitivity Magnetic Field Sensor*, Sensors a. Actuators, 2000, **85**, 202–208.
5. R. S. Popovic, *Not-Plate-Like Hall Magnetic Sensors and Their Applications*, Sensors a. Actuators, 2000, **85**, 9–17.
6. G. Boero, M. Demierre, P. A. Besse, R. S. Popovic, *MicroHall Devices: Performance, Technologies and Applications*, Sensors a. Actuators A, 2003, **106**, 314–320.
7. Ichiro Shibasaki, *Mass Production of InAs Hall Elements by MBE*, J. Crystal Growth, 1997, **175/176**, 13–21
8. M. Behet, J. De Boeck, G. Borghs, P. Mijlemans, *Comparative Study on the Performance of InAs/$Al_{0.2}Ga_{0.8}Sb$ Quantum Well Hall Sensors on Germanium and GaAs Substrates*, Sensors a. Actuators, 2000, **79**, 175–178.
9. Ch. S. Roumenin, D. Nikolov, A. Ivanov, *A Novel Parallel Field Hall Sensor with Low Offset and Temperature Drift Based 2D Integrated Magnetometer*, Sensors a. Actuators A, 2003, **115**, 303 – 307.
10. T. Przesławski, A. Wolkenberg, K. Regiński, J. Kaniewski, *Heterojunction $In_{0.53}Ga_{0.47}As$/InP Magnetic Field Sensors Fabricated by Molecular Beam Epitaxy*, Optica Appl., 2002, **XXXII**, 511–515.
11. T. Przesławski, A. Wolkenberg, K. Regiński, J. Kaniewski, *Sensitive $In_{0.53}Ga_{0.47}As$/InP(SI) Magnetic Field Sensors*, phys. stat. sol. (c), 2004, **1**, 242–246.
12. J. Heremans, *Solid State Magnetic Field Sensors and Applications*, J. Phys. D: Appl. Phys., 1993, **26**, 1149–1168.
13. J. Heremans, *Narrow-Gap Semiconductor Magnetic Field Sensors and Applications*, Semicond. Sci. Technol.,1993, **8**, S424–S430.
14. H. J. Lippmann, F. Kuhrt, *Der Geometrieeinfluss auf den transversalen magnetischen Widerstandseffekt bei recht-*

förmigen Halbleiterplatten, Z. Naturforsch. 1958, **13A,** 462–483.
15. R. S. POPOVIC, *Hall Effect Devices*, Bristol, Adam Hilger 1991.
16. J. HAEUSLER, H. J. LIPPMANN, *Hallgeneratoren mit kleinem Linearisierungsfehler*, Solid State Electron., 1968, **11**, 173–182
17. A. KOBUS, J. TUSZYŃSKI, *Hallotrony i gaussotrony*, WNT, Warszawa 1966.
18. E. PETTENPAUL, J. HUBER, H. WEIDLICH, W. FLOSSMANN, U. VON BORCKE, *GaAs Hall Devices Produced by Local Ion Implantation*, Solid State Electron., 1981, **24**, 781–786.
19. H. P. BALTES, R. S. POPOVIC, *Integrated Semiconductor Magnetic Field Sensors*, Proc. IEEE, 1986, **74**, 1107–1132.
20. R. S. POPOVIC, *Hall-Effect Devices*, Sensors a. Actuators, 1989, **17**, 39–53.
21. R. S. POPOVIC, J. A. FLANGAN, P. A. BESSE, *The Future of Magnetic Sensors*, Sensors a. Actuators, 1996, **A56**, 39–55.
22. V. P. KUNETS,W. HOERSTEL, H. KOSTIAL, H. KISSEL, U. MULLER, G. G. TARASOV, Y. I. MAZUR, Z. YA. ZHUCHENKO, W. T. MASSELINK, *High Electric Field Performance of $Al_{0.3}Ga_{0.7}As$/GaAs and $Al_{0.3}Ga_{0.7}As$/GaAs/ $In_{0.3}Ga_{0.7}As$ Quantum Well Micro-Hall Devices*, Sensors a. Actuators, 2002, **A101**, 62–68.
23. A. WOLKENBERG, T. PRZESŁAWSKI, J. KANIEWSKI, J. BĄK-MISIUK, K. REGIŃSKI, *Thickness Dependence of the Structural and Electrical Properties of InAs Layers Epitaxially Grown by MBE on GaAs (001)*, Mater. Sci. Eng. 2000, **B 77**, 250–254.
24. A. NEDOLUHA, K. M. KOCH, *Zum Mechanismus der Widerstandsänderung im Magnetfeld*, Z. für Physik, 1952, **132**, 608–620.
25. H. H. WIEDER, *Transport Coefficients of InAs Epilayers*, Appl. Phys. Lett., 1974, **25**, 206–208.
26. P. D. WANG, S. N. HOLMES, TAN LE, R. A. STRADLING, I. T. FERGUSON, A. G. DE OLIVEIRA, *Electrical and Magneto-optical Studies of MBE InAs on GaAs*, Semicond. Sci. Technol., 1992, **7**, 767–786.
27. E. W. SAKER, F. A. CUNNELL, J. T. EDMOND*, Indium-Antimonide as a Fluxmeter Material*, British J. Appl. Phys. 1955, **6**, 217–220.
28. S. KATAOKA, H. YAMADA, Y. SUGIYAMA, H. FUJISADA, *New Galvanomagnetic Device with Directional Sensitivity*, Proc. IEEE, 1971, **B59**, 1349–1349.